CHAPTER IV
RESULTS AND DISCUSSION

4.1 Electrospinning Solution

Poly(vinyl alcohol) (PVA) nanofibers containing platinum and ruthenium nanoparticles have been obtained by electrospinning a solution containing platinum and ruthenium nanoparticles. Chloroplatinic acid hexahydrate ($H_2PtCl_6.6H_2O$) and ruthenium chloride ($RuCl_3.xH_2O$) as precursors were reduced directly in PVA viscous solution by citrate ions under 95-100 °C and vigorous stirring, then PVA protected the platinum and ruthenium nanoparticles. The platinum and ruthenium precursors, chloroplatinic acid hexahydrate ($H_2PtCl_6.6H_2O$) and rutheniumchloride ($RuCl_3 \cdot xH_2O$), were reduced to Pt and Ru metal particles directly in 8% PVA viscous solution by citrate ions (Lin *et al.*, 2005) under 95-100 °C and vigorous stirring as follows:

$$PtCl_6^{2-} + Cit^- + H_2O \rightarrow Pt^0 + CO_2 + H^+ + Cl^- \quad (4.1)$$

$$Ru^{3+} + Cit^- + H_2O \rightarrow Ru^0 + CO_2 + H^+ + Cl^- \quad (4.2)$$

However, PVA fine powder was added twice. Mainly because the viscosity of solution increased if all the PVA as added to the system directly at once, the reaction between chloroplatinic acid, ruthenium chloride and reducing agent was decreased, and the nanoparticles could not be well dispersed in the PVA solution. Firstly, small amount of PVA added served as a stabilizer to prevent an aggregation of Pt–Ru nucleuses generated during chemical reduction. Later, more PVA was added in order to form fiber formations. In addition, if large amount of PVA was added at once, long PVA chains (molecular weight = 72,000) would restrict chemical reaction between chloroplatinic acid hexahydrate, ruthenium chloride and citrate ions giving small content of Pt–Ru nanoparticles (Bai *et al.*, 2007).

PVA has high viscosity due to the strong intermolecular hydrogen bondings between PVA chains and water molecules. The strong intramolecular hydrogen bondings between hydroxyl groups on the same PVA chains also have the effect on the solution viscosity. In addition, PVA applied in the experiment had high

molecular weight (72,000) which could cause high degree of entanglement (Chang *et al.*, 2005). As Pt–Ru metal occurred in the system, the solution concentration was increased. Moreover, the attraction force between Pt–Ru nanoparticles and lone pair electron of hydroxyl groups on PVA chains took place promoting the viscosity of the solution. Therefore, the viscosities of the solution were increased when increasing amounts of Pt–Ru precursors as shown in table 4.1.

Table 4.1 The viscosities of solutions with different Pt–Ru loadings

Pt–Ru loading (wt %)	0	0.36	1.07	1.79
Average Viscosity (cP)	191.0 ± 1.26	207.2 ± 3.31	239.2 ± 1.67	299.8 ± 5.38

Figure 4.1 shows UV–visible absorption spectra of aqueous solution of PVA stabilized at different concentrations of Pt–Ru precursors including 0.36%, 1.07% and 1.79% Pt–Ru loadings before reduction reaction took place. The spectra exhibits an absorption band at around 260-265 nm suggesting the formation of Pt^{4+} contained in each solution. The Ru^{3+} absorption spectra shows very small peak at ~436 nm as a result of the small amount of $RuCl_3$ precursor (Liu *et al.*, 2007). It was found that the intensity of the absorption band increased when the concentration of precursors increased (Lin *et al.*, 2006).

Figure 4.2 demonstrates the UV absorption property of prepared solution with 0.36% Pt–Ru loading at different reduction time. At 0 minute or before reaction started, the absorption band appeared at 260 nm and 436 nm in its UV-vis spectrum as a result of Pt^{4+} and Ru^{3+} in the solution as mentioned above. On the other hand, when reduction reaction with citrate salts had taken place after 30 minutes, the bands at 260 nm and 436 nm are no longer visible which suggested that $H_2PtCl_6.6H_2O$ and $RuCl_3.xH_2O$ were completely reduced to metal forms. In addition, the particles suspended and stabilized in the aqueous solution as dark brown solution was obtained. The spectrum of the completely reduced solution displays strong absorption from 700 nm and a gradually increasing intensity from the visible to the ultraviolet region due to larger amount of Pt–Ru particles produced in the system scattered the UV radiation provided (Liu *et al.*, 2007) In addition, the bands tended to

increase towards the shorter wavelengths in UV range due to the surface plasmon of platinum and ruthenium nanoparticles (Chen *et al.*, 2007).

Figure 4.3 and 4.4 illustrate the UV absorption property of prepared solution with 1.07% and 1.79% Pt–Ru loadings at different reduction time. The results were similar to those observed in 0.36% Pt–Ru loading. Furth ermore, in figure 4.5-4.8, the higher UV absorption bands were obtained by increasing amount of precursors at different reaction time according to more Pt–Ru nanoparticles were generated in the systems.

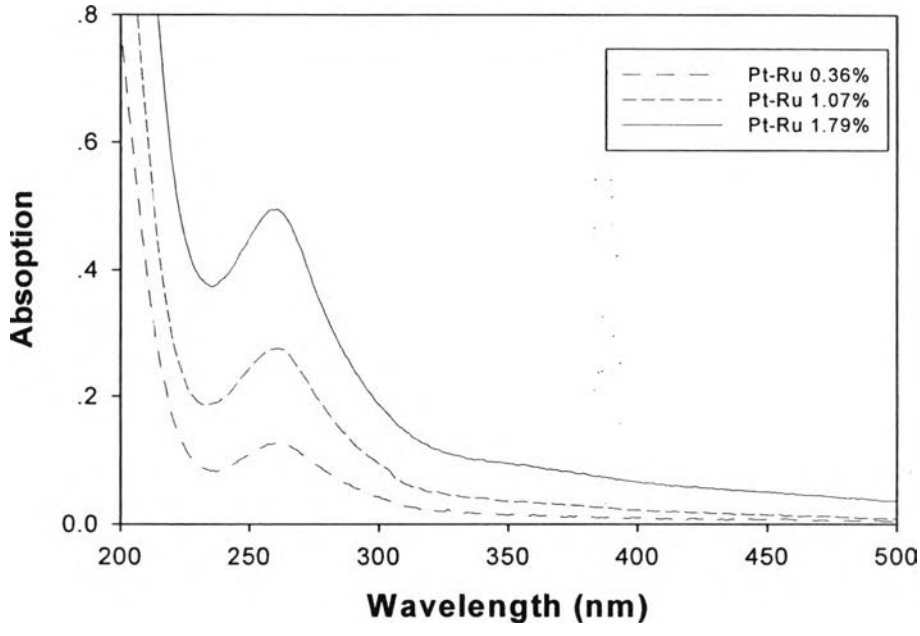

Figure 4.1 UV-visible absorption spectra of aqueous solution of PVA stabilized at different Pt–Ru loadings 0.36%, 1.07%, and 1.79% before chemical reduction.

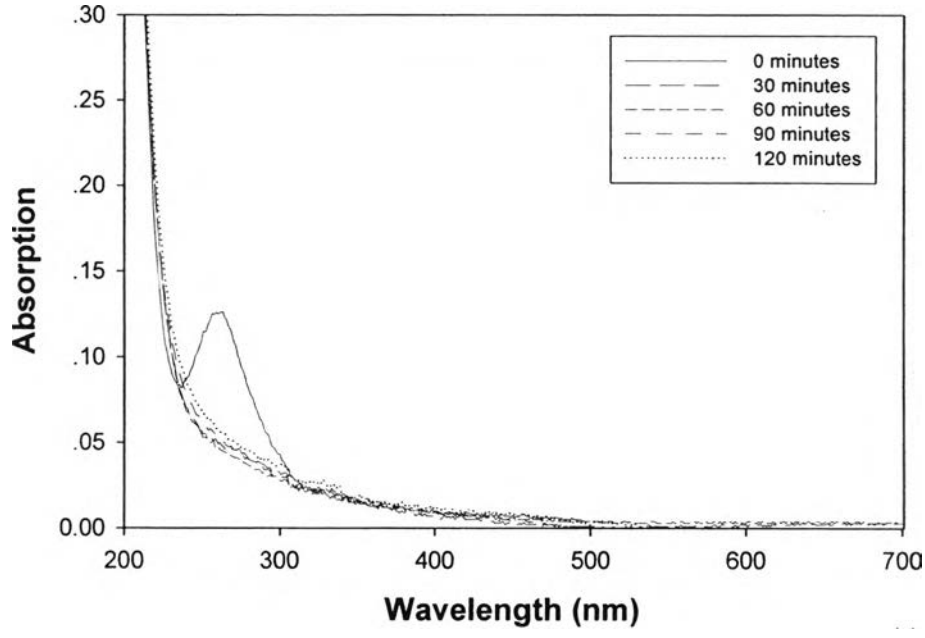

Figure 4.2 UV-visible absorption spectra of aqueous solution of 0.36%wt Pt–Ru loading at different time.

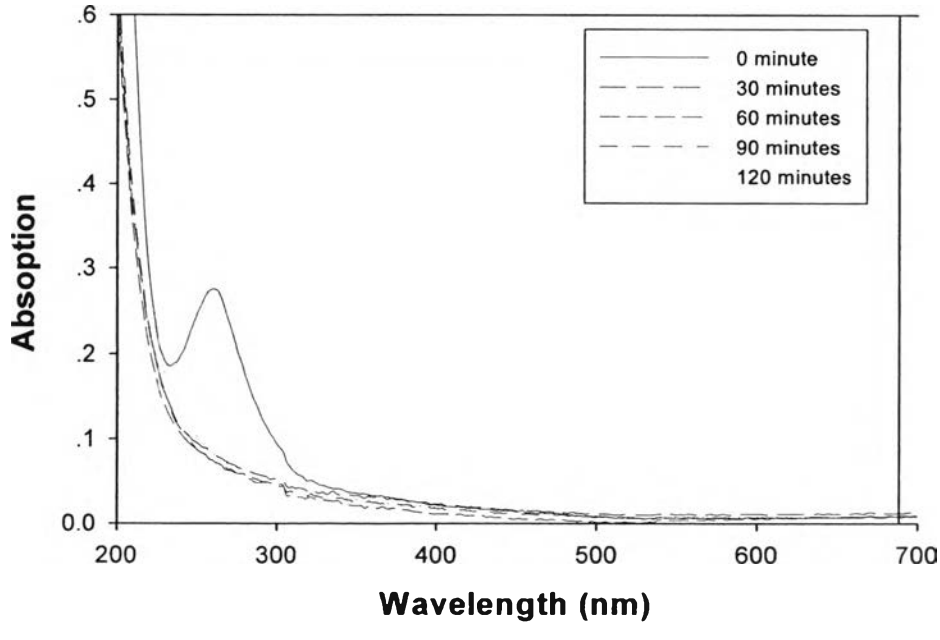

Figure 4.3 UV-visible absorption spectra of aqueous solution of 1.07% Pt–Ru loading at different time.

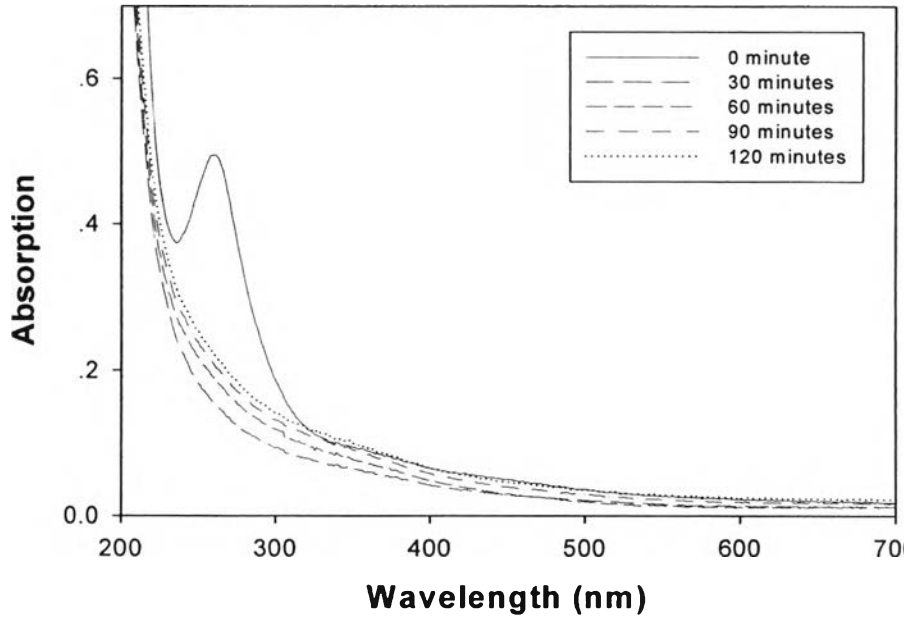

Figure 4.4 UV-visible absorption spectra of aqueous solution of 1.79 % Pt–Ru loading at different time.

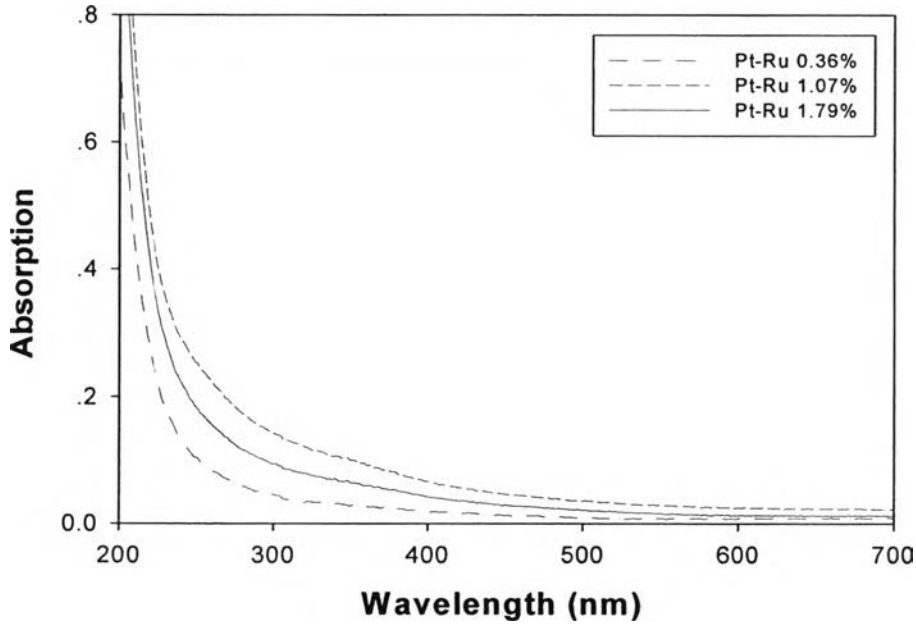

Figure 4.5 UV-visible absorption spectra of aqueous solution of PVA stabilized at different Pt–Ru loadings after 30 minutes.

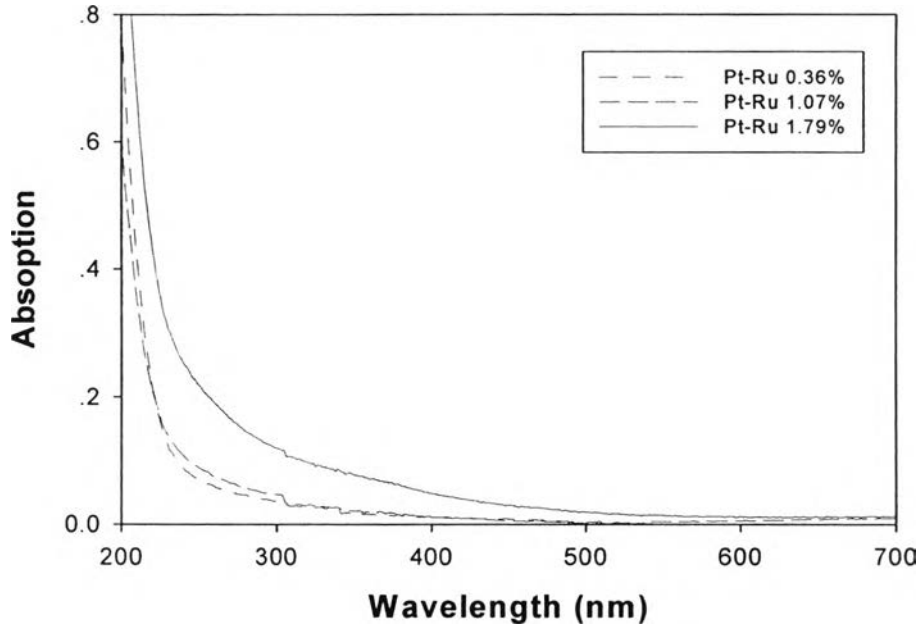

Figure 4.6 UV-visible absorption spectra of aqueous solution of PVA stabilized at different Pt–Ru loadings after 60 minutes.

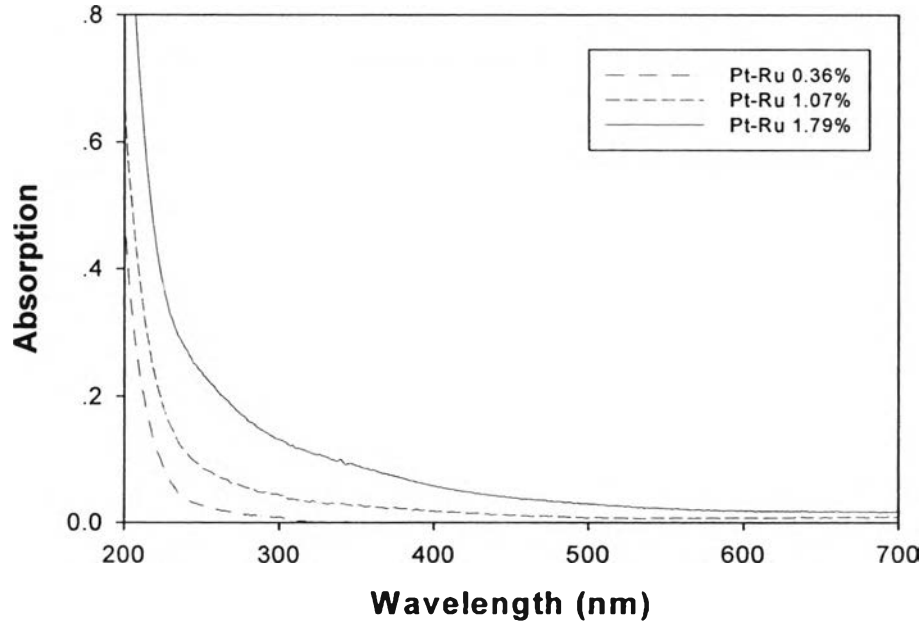

Figure 4.7 UV-visible absorption spectra of aqueous solution of PVA stabilized at different Pt–Ru loadings after 90 minutes.

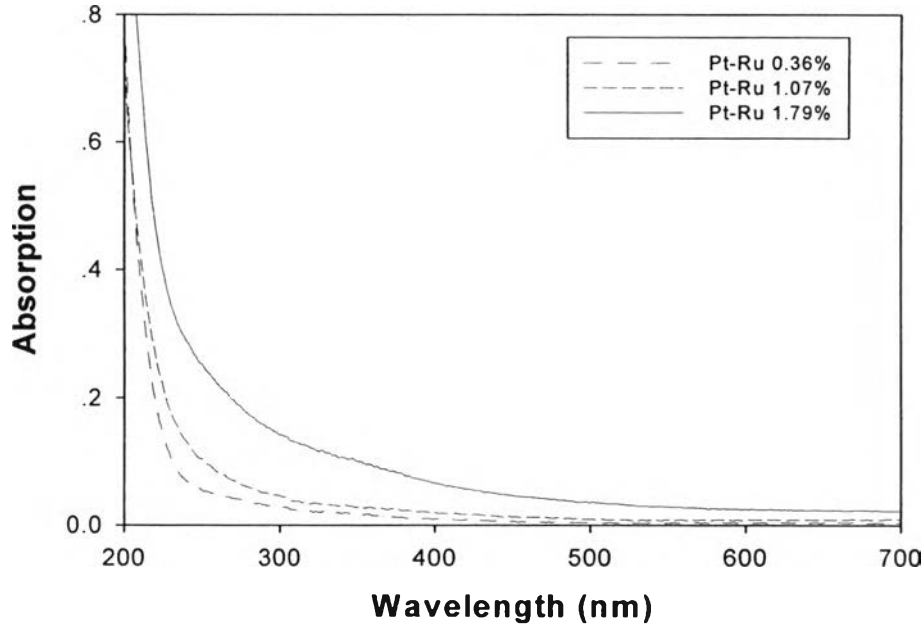

Figure 4.8 UV-visible absorption spectra of aqueous solution of PVA stabilized at different Pt–Ru loadings after 120 minutes.

The electrical conductivities of the PVA/Pt–Ru solutions at room temperature were observed by conductivity meter. The results were shown in figure 4.9. The contents of Pt–Ru nanoparticles were 0.36%, 1.07% and 1.79%, the conductivities of the solution are 1.214 mS/cm, 1.340 mS/cm and 1.4080 mS/cm respectively. It was found that the conductivities of solution were increased with increasing amounts of Pt–Ru in solution. As a result of platinum and ruthenium are good conductors, they are beneficial for improving the conductivity of PVA solution when they disperse in the solution (Bai *et al.*, 2007).

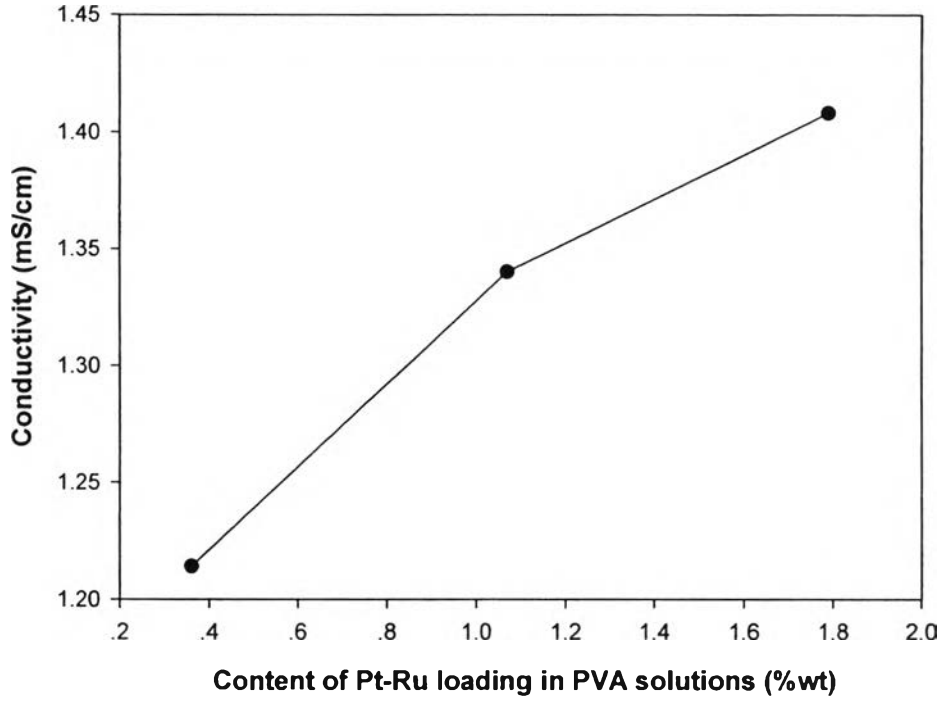

Figure 4.9 Electrical conductivities of different Pt–Ru loadings in PVA solution.

4.2 Morphology

The average diameter of the nanofibers were obtained from SEM images in figure 4.10 ranging from 234 to 166 nm calculated by Semafore. For the pure PVA, an average diameter was 166.6 nm. For Pt–Ru loading of 0.36%, 1.07% and 1.79% average diameters were 234.4 nm, 199.8 nm and 180.1 nm, respectively. The results were given in the table 4.2. The results show that the average diameters were decreased with increasing amounts of Pt–Ru precursor. The result corresponded to increasing of charge density when more precursors were added. Since platinum and ruthenium are good conductors, they are beneficial for improving the conductivity of PVA solution when they disperse in the solution. The higher conductivity can induce the stronger elongation of the ejection of the electrospinning solution to the metal collector and let to smaller fiber formation (Bai *et al.*, 2007).

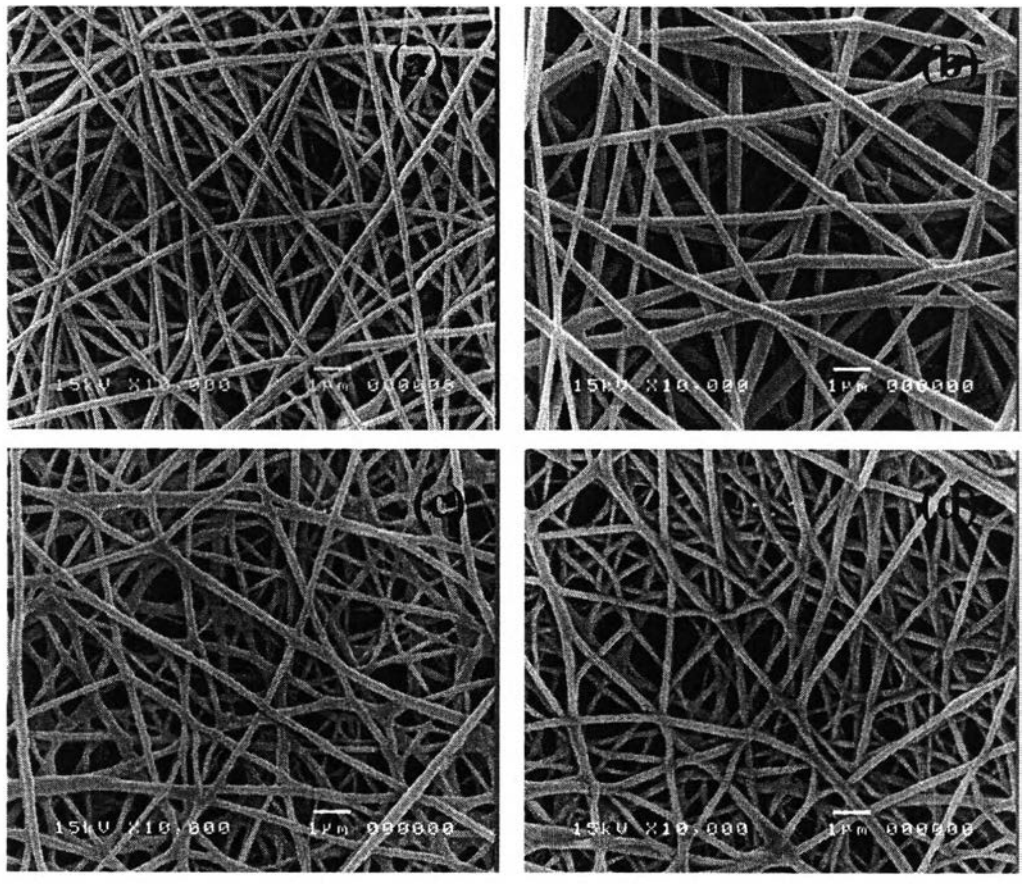

Figure 4.10 SEM images of composite fibers with different %Pt–Ru loadings (a) pure PVA, (b) 0.36%, (c) 1.07%, and (d) 1.79%.

In the figure 4.10, the fusions of fibers were observed according to some moisture in the atmosphere since PVA is water-soluble polymer. To solve this problem, the nanofibers have to be treated with glutaraldehyde before heat crosslink the nanofibers. Then the PVA nanofibers become water-insoluble (Shan *et al.*, 2007).

Table 4.2 Average diameters of as-spun fibers from different % Pt–Ru loadings

% Pt–Ru loading	0	0.36	1.07	1.79
Average Diameter (micron)	0.1666 ± 0.025	0.2344 ± 0.044	0.1998 ± 0.035	0.1801 ± 0.023

The histograms of PVA nanofiber size distributions were plotted in the figure 4.11. The results show that the 1.79% Pt–Ru loading gave the narrowest size distribution of the PVA nanofibers containing Pt-Ru nanoparticles.

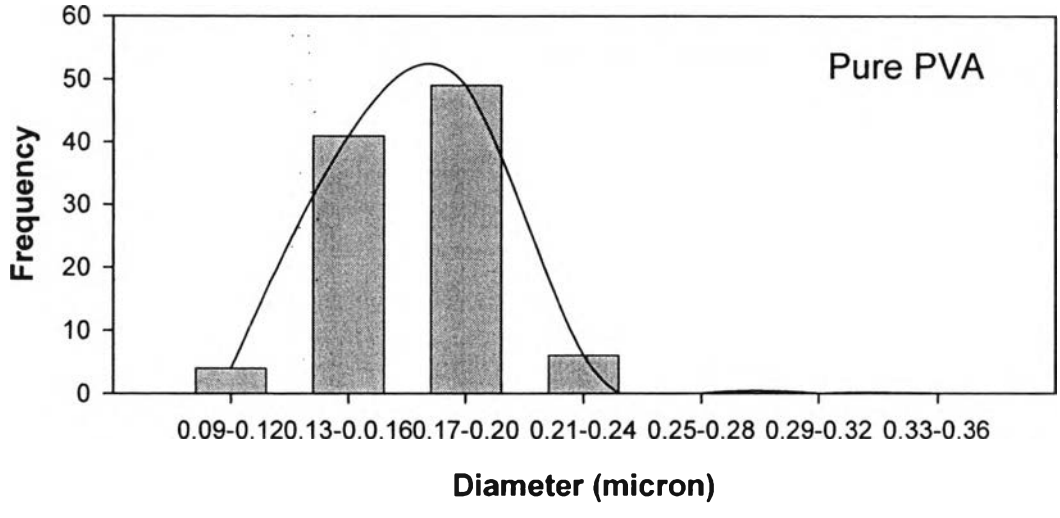

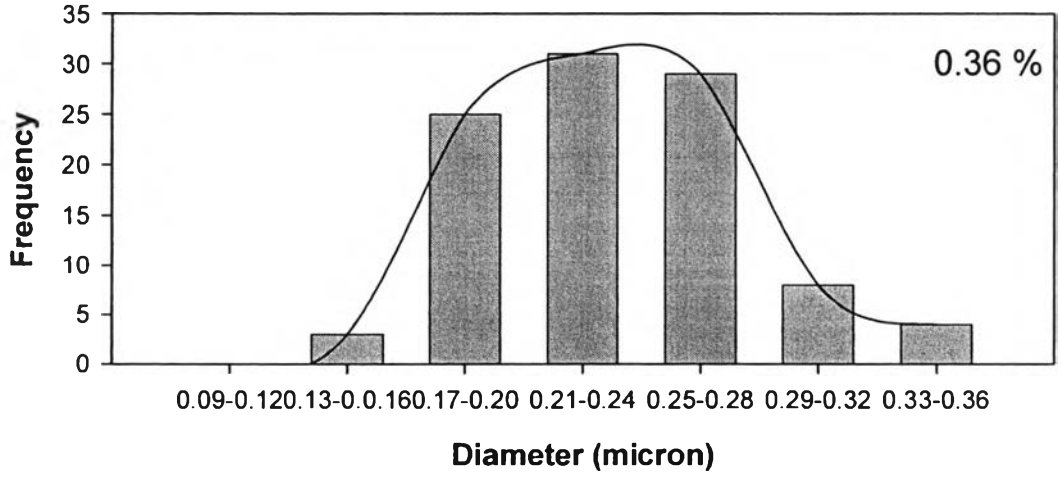

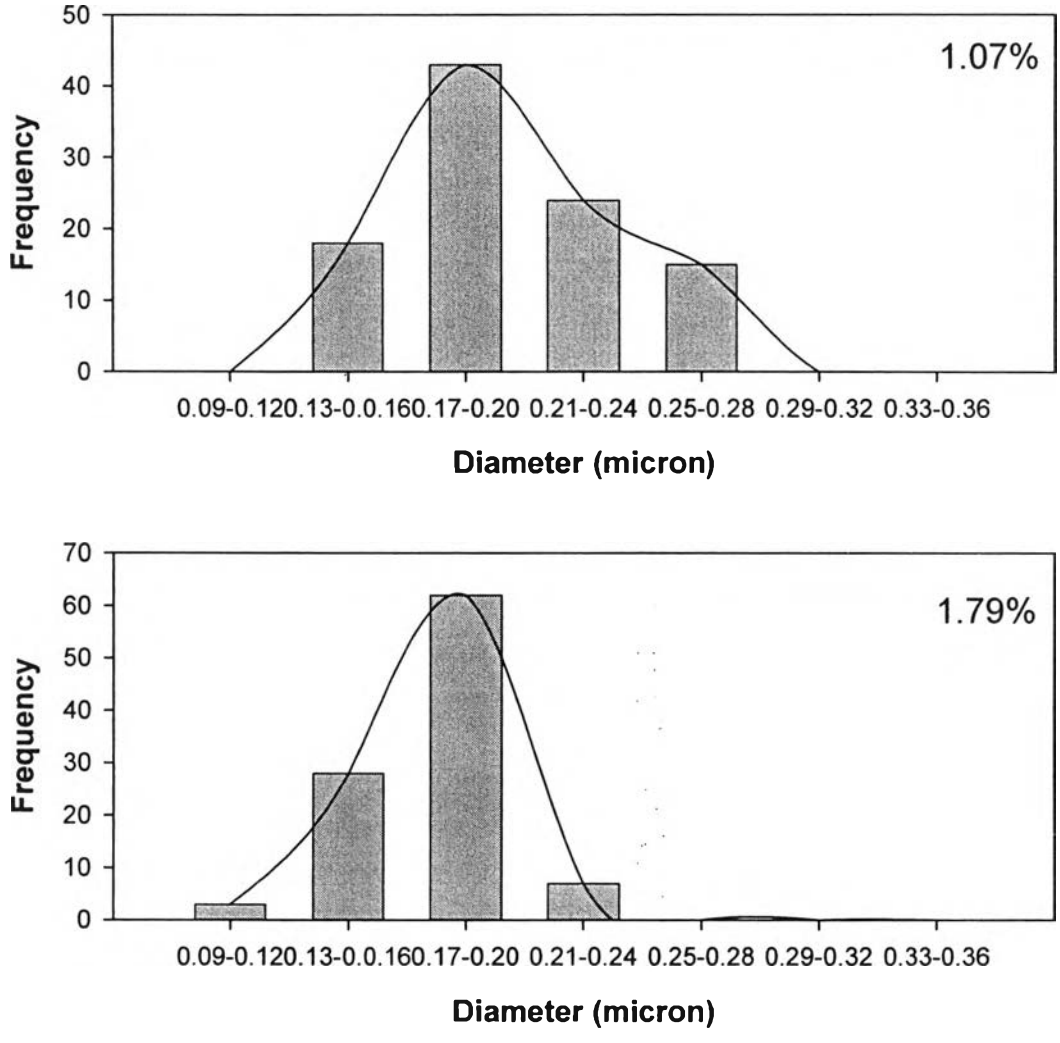

Figure 4.11 Histograms of size distribution nanofiber of Pure PVA, 0.36%, 1.07% and 1.79% Pt–Ru loadings.

The SEM technique was inadequate to investigate on Pt–Ru nanoparticles inside the fibers, therefore, the TEM technique was then required. The images of the PVA nanofibers electrospun from the 8 % PVA aqueous solutions containing Pt and Ru nanoparticles are presented in figure 4.12. As a result of the increasing in chloroplatinic acid hexahydrate and ruthenium chloride content, more Pt–Ru particles were produced in the fibers. From the excess of reducing agent, tri-sodium citrate, more precursors added can also be reduced completely giving larger amount of the particles generated in the fibers. The pure PVA had bright color compared to

0.36%, 1.07% and 1.79% which show some darker zones which were believed to be groups of individual Pt–Ru nanoparticles. The average size of the Pt and Ru nanoparticles in the PVA nanofibers electrospun was in range 2 to 5 nm. The results illustrate that the average diameters of Pt and Ru particles change with the different concentrations of chloplatinic acid and ruthenium chloride precursors.

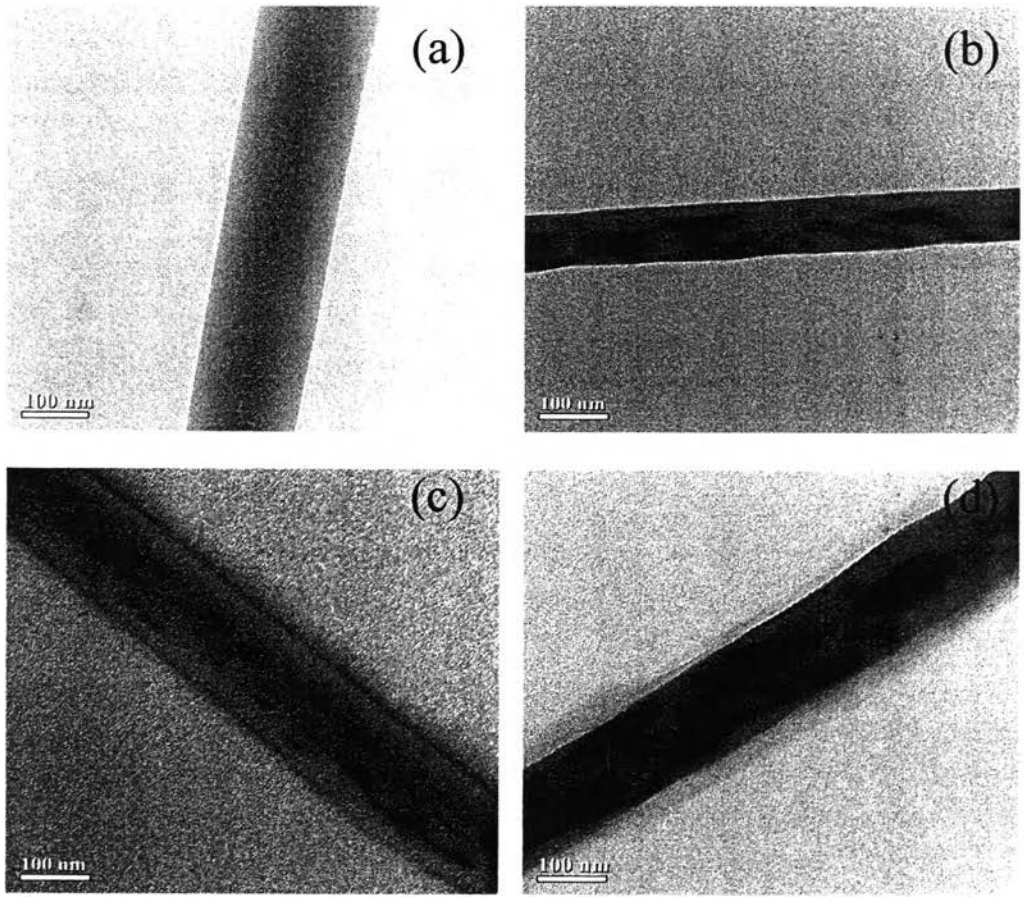

Figure 4.12 TEM images of Pt–Ru incorporated nanofibers from pure PVA and PVA templates with different % Pt–Ru loadings; (a) pure PVA, (b) 0.36%, (c) 1.07%, and (d) 1.79%.

4.3 Characterization of Pt–Ru Nanoparticles

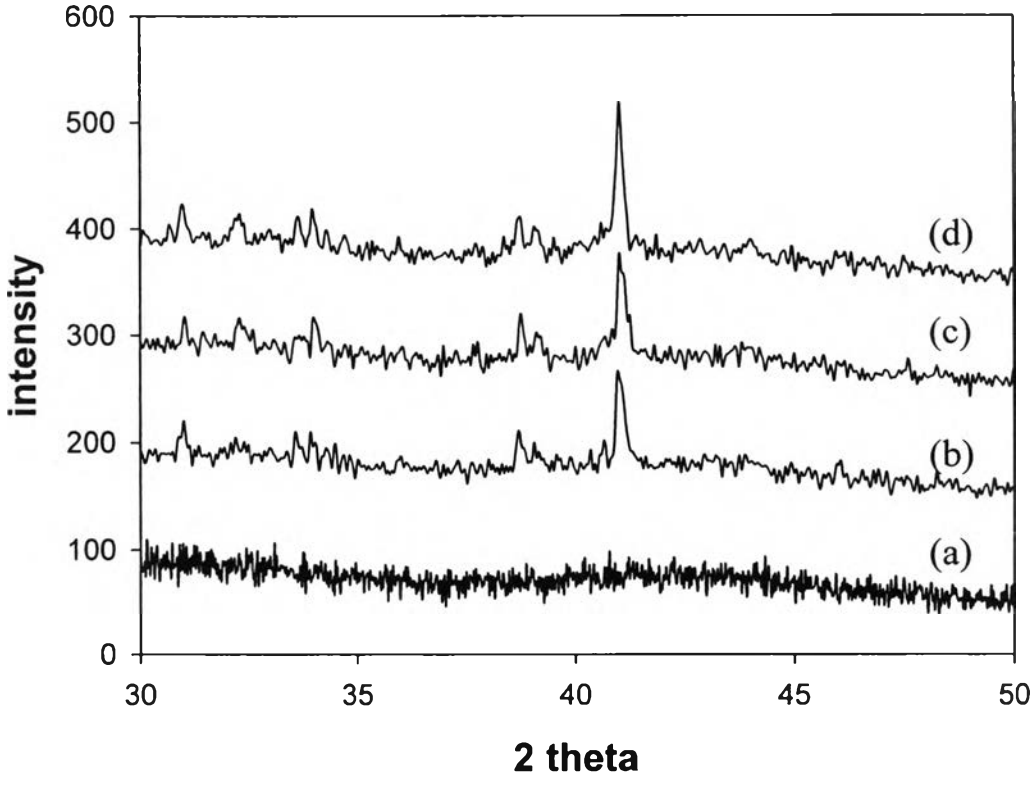

Figure 4.13 XRD pattern of pure PVA mat and PVA nanofibers with different Pt–Ru loadings: (a) pure PVA, (b) 0.36%, (c) 1.07%, and (d) 1.79%.

The way to confirm the occurrence of Pt and Ru elements in the PVA nanofiber mats is XRD. Figure 4.13 illustrates the XRD pattern of the as prepared PVA/Pt–Ru electrocatalyst. The diffraction peaks were ascribed to (1 1 1), (2 0 0), (3 1 1) planes of face-centered cubic (fcc) crystal of the nanoparticles. As the Pt–Ru content increased, the intensity of the peak gradually increased. It was reported that when some of the platinum atoms in the fcc crystal structure are replaced by the smaller ruthenium atoms, the diffraction peaks slightly shift to higher angles. Since the peaks of the nanoparticles in figure 4.13 were located at the angles higher than those of pure Pt (Nagao *et al.*, 2006). However, the resultant characteristic peaks are not sharp, which indicates a somewhat amorphous structure for the catalyst. In

addition, no apparent peaks corresponding to the hcp phases of the Ru element can be seen. This phenomenon is commonly found for supported Pt–Ru electrocatalysts except those of the highly Ru-rich particles. It can be attributed to the coincidence that the signal peaks of both Pt and Ru elements appear at almost the same positions. The Pt element has a much larger size. Therefore, it exhibits a more pronounced signal pattern than that of the Ru counterpart (Hsu *et al.*, 2008).

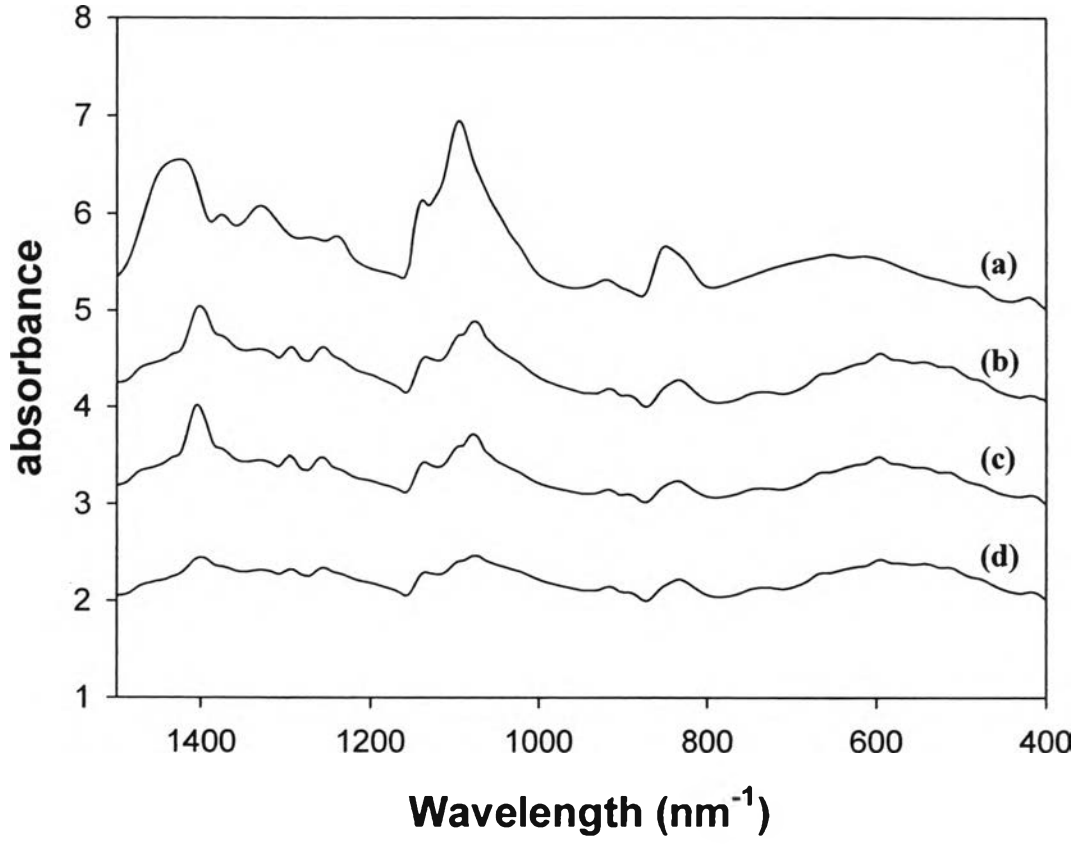

Figure 4.14 FTIR spectra of pure PVA mat and PVA nanofibers with different Pt–Ru loadings: (a) pure PVA, (b) 0.36%, (c) 1.07%, and (d) 1.79%.

The FTIR spectra of as prepared nanofibers illustrate the chemical bonding between the PVA matrix and the Pt–Ru nanoparticles taking place. According to the FTIR spectra in figure 4.14, the pure PVA and the PVA/Pt–Ru nanocomposites with different loading of Pt–Ru were compared. The band at 617 cm^{-}, out-of-plane vibration of O-H groups, which quite board in normal alcohol and the band at 849

cm-1 which referred to C-H bonds that vibrates out-of-plane, these bands decreased as adding more Pt-Ru loading. Moreover, absorption bands at 1331 cm^{-1} and 1418 cm^{-1} which respectively belonged to the coupling of O-H in plane vibration and C-H wagging vibrations were slightly weakened when increasing the amount of Pt–Ru loading (Bai *et al.*, 2007). This indicates that interaction between PVA matrix and Pt–Ru nanoparticles took place over the O-H groups. In addition, the peak positions detected slightly shifted to smaller wavelength according to the interaction between Pt–Ru particles and support molecules. However, the limit of the instrument may could causes the decreasing of the band in pure PVA compared to PVA/Pt–Ru composite nanofibers.

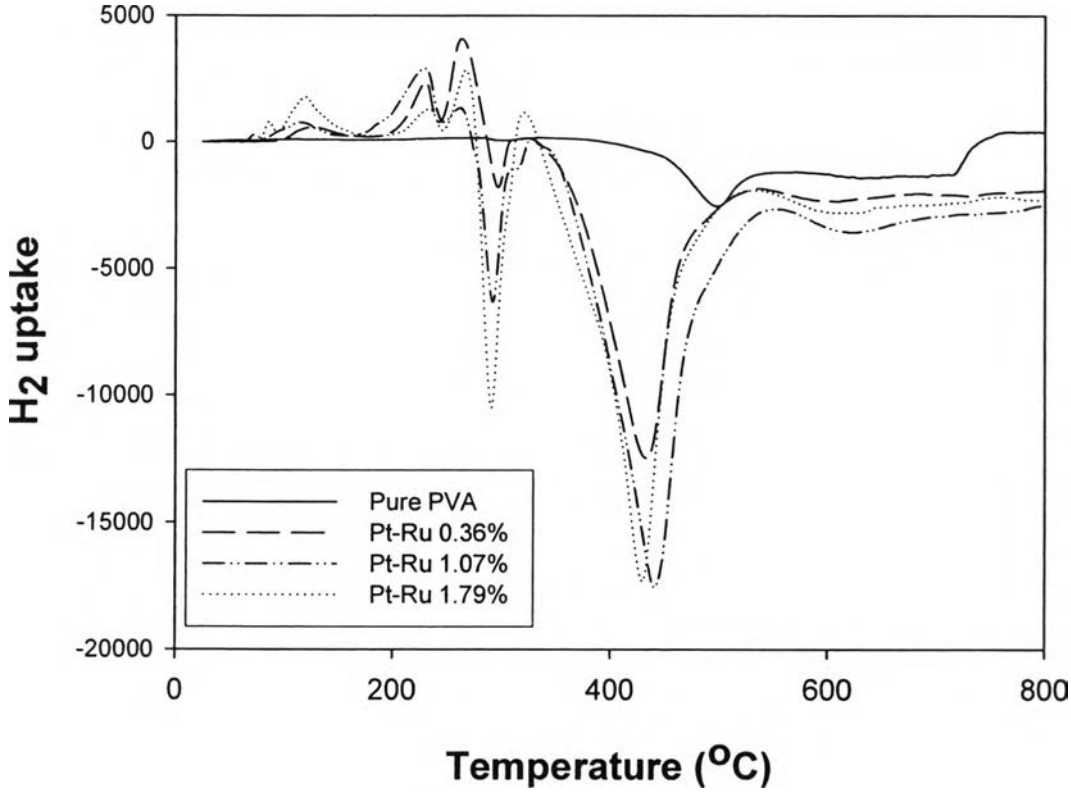

Figure 4.15 TPR of pure PVA and PVA with different Pt–Ru loadings.

Figure 4.15, a pure PVA and nanocomposite nanofiber flakes were heated under hydrogen atmosphere from 30-700 °C. The pure PVA gave a flat line before 350 °C was reached. No hydrogen was absorbed; instead, pure PVA gave out some

hydrogen gas after 350 °C according to the degradation of PVA at elevated temperature. The hydrogen absorption peaks about 100 °C and 200 °C of nanocomposite nanofibers with 0.36%, 1.07% and 1.79% Pt–Ru loadings attributed to the reduction of Pt–Ru nanoparticle (Kim *et al.*, 2008). Also hydrogen desorption peaks were observed at about 300 °C and 445 °C. A small reduction peak at about 100 °C followed by a broader main peak centered at 200 °C were observed for PVA/ Pt–Ru due to the reduction of platinum and ruthenium oxide generated from being oxidized by oxygen in the atmosphere during electrospinning process. From Pieck et al. (2001), the TPR spectra of PtO_x and RuO_x usually exhibit two reduction peaks at about 100 °C and 200 °C. However, the peak positions detected slightly shifted according to the interaction between Pt–Ru particles and support molecules. Therefore, some Pt and Ru ions were completely reduced from $Pt^{4+}$and Ru^{3+} to either metal form or oxide form. Pt and Ru in oxide form were reduced again by hydrogen gas supplied and transferred to metal form eventually. The desorption peaks, at 300 °C and 445 °C, were also corresponding to the degradation of the PVA templates supporting Pt–Ru nanoparticles.

Thermogravimetric analysis was applied to investigate thermal property of the nanocomposites nanofibers, degradation behavior, under heating rate of 10 °C min^{-1}. Temperature was swept from 50-600 °C under N_2 atmosphere. From 50-100 °C, the thermograms (figure 4.16) showed the loss of water which water content was high in PVA containing Pt–Ru nanoparticles, whereas a small amount of water elimination in pure PVA was observed. The loss was due to some moisture contained on the fiber mats as PVA is a water-soluble polymer. Pure PVA and the nanocomposite nanofibers exhibited 2-step degradation (Peng and Kong, 2007). The first step degradation in pure PVA (250-350 °C) involves chain stripping elimination of H_2O and the chain-scission reactions which occur in parallel. The products of the first step are polyenes from the chain-stripping elimination reaction of H_2O, also *cis* and *trans* allylic-methyls that may form from random chain scission that takes place with an elimination. The second step (450-550 °C), cyclization (Diels-Alder intramolecular and intermolecular cyclization followed by dehydrogenation with aromatization) and radical reaction pathways, which occur in parallel, are responsible

for the conversion of unsaturated carbons into substituted aromatic or aliphatic carbons (Krklješ *et al.*, 2007).

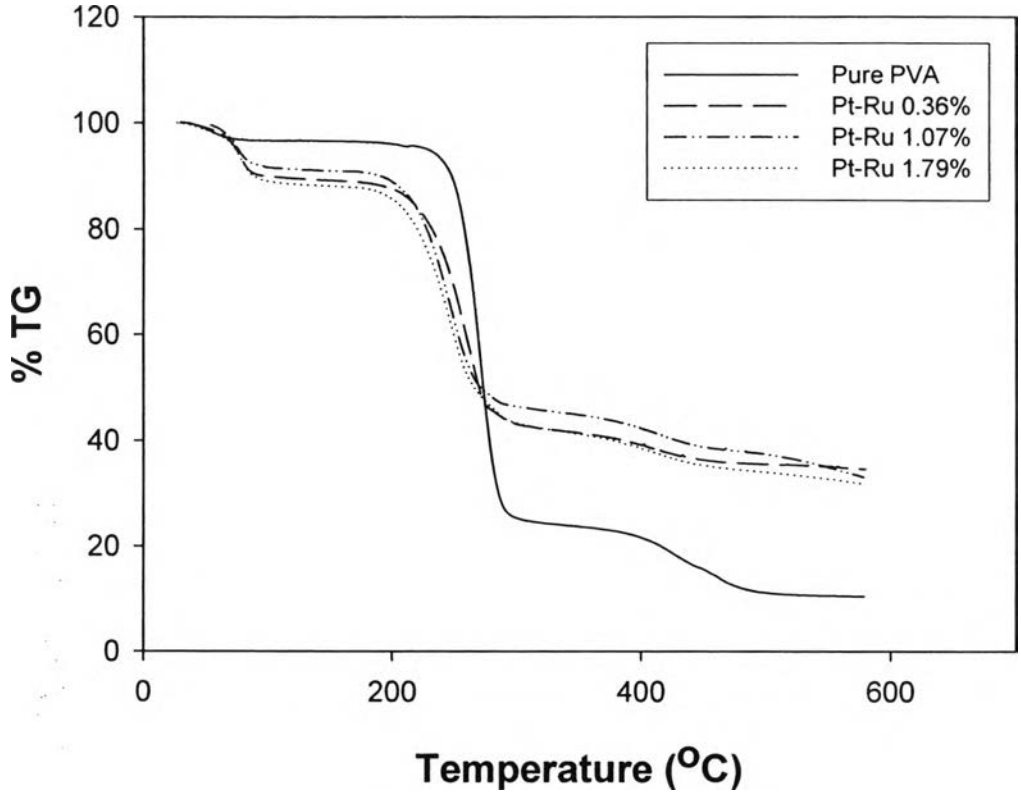

Figure 4.16 TGA thermograms of pure PVA and PVA with different Pt–Ru loadings.

Two general mechanisms are probably responsible for the modes of action of Pt–Ru nanoparticles on the thermal degradation of PVA. One is described as a chemical constraint for the H_2O elimination in the first degradation step due to the interaction of Pt and Ru nanoparticles with OH groups, which may increase energy barrier of the chain-stripping elimination reaction of H_2O and induce a shift of the thermal degradation of partial decomposition products toward chain scission and formation of methyl terminated polyenes. In addition, the interaction of OH groups with Pt–Ru nanoparticles is confirmed by FTIR spectra which were discussed earlier. Pt–Ru nanoparticles may act as radical scavenger suppressing radical transfer to the adjacent chains via intermolecular and intramolecular chain reactions. The second

mechanism is a physical constraint (reduced molecular mobility) for the reactions of inter and intra cyclization of polyenes in the second degradation step that seem to occur preferably at a lower heating rate compared with radical reaction pathways.

Table 4.3 Pt–Ru content in each fiber mat obtained from XRF-EDX spectrum

% Pt–Ru loading	0	0.36	1.07	1.79
average Pt content in a fiber mat (ppm)	0.0 ± 0.0	632.3 ± 39.2	1040.7 ± 55.6	2946.9 ± 177.5
average Ru content in a fiber mat (ppm)	0.0 ± 0.0	40.0 ± 5.0	52.0 ± 3.6	135.7 ± 6.0

From XRF-EDX results in table 4.3, it was found that 0.36%, 1.07% and 1.79% Pt–Ru loadings gave Pt nanoparticles content of 632.3, 1040.7, and 2946.3 ppm respectively. Moreover, the Ru content of 0.36%, 1.07% and 1.79% Pt–Ru loadings are 40.0, 52.0, and 135.7 ppm, respectively. As a result of the increasing in precursor content caused larger Pt–Ru nanoparticles composition on the PVA fiber mats.